PAUL SCHERRER INSTITUT

SWISS LIGHT SOURCE SLS

SLS-TME-TA-2003-0223
17th June 2004

SLS-FEMTO: Chicane layout, performance and side-effects

Andreas Streun

Paul Scherrer Institut, CH-5232 Villigen PSI, Switzerland

After a summary of previous work the final layout of the SLS-FEMTO insertion is described covering magnet parameters, geometric layout and matching conditions. Negative side-effects affecting transverse acceptance, beam lifetime and storage ring emittance are discussed as well as flexibility and performance of the chosen scheme.
The relation between emittance increase and angle of separation between short pulse and core beam radiation is investigated in detail revealing the guidelines for the optimum choice of parameters.

1 Summary of previous work

In a previous paper from May 2002 [9] different separation schemes for the SLS-FEMTO insertion were discussed: The available options were separation in the vertical plane exploiting the smaller vertical beam size or in the horizontal plane, using a stronger chicane; further the separation could be done spatially with a point to point X-ray optics for imaging the separated beams to the experiment, or angular without any optics just letting the beams drift away from each other.

- **Vertical angular** separation was rejected immediately, since the separation required to get the satellite beam out of the core photon beam's side lobes would spoil completely the vertical emittance.

- **Vertical spatial** separation was favoured for quite a while [4], however eventually it was rejected for several problems, above all that no solution was found how to block or guide out the modulator beam. Further the feasibility of the X-ray optics required for imaging on micron scales was not proven.

- **Horizontal angular** separation turned out to be the most promising scheme. First simulations of the photon beams indicated that the satellites could be well extracted from the core beam. Also the problem of modulator beam blocking was solvable. Main side-effect was almost doubling of the storage ring emittance.

- **Horizontal spatial** separation had not been treated but was considered as promising too, since the X-ray optics for imaging would work on larger scales and thus be less sensitive to imperfections of the mirrors.

Since then work progressed further on photon beam simulations, magnet and vacuum chamber designs and electron beam dynamics:

- Originally, it was planned to use energy separation, i.e. exploit the characteristics of the undulator spectrum and use the satellite beam with positive energy offset, which would have required to build the modulator chicane pointing to the inside of the storage ring. Recent calculations [2] showed, that the background from modulator, chicane dipoles and ring bending magnets can be better suppressed with the chicane pointing to the outside, with it using the negative satellite.

- Also technological and geometric considerations were in favour of a chicane to the outside of the ring: Coupling in the laser and blocking the modulator beam or even guiding it out would be much easier.

- The modulator design was changed in favour of lower field and larger period. As will be explained below, this gives less ring emittance increase of approx. 40 % instead of almost 100 % as before. Since the number of periods is given,

more length had to be reserved for the modulator. The latest considerations are based on a hybrid type undulator. An alternative solution would include a superconducting device with first and second chicane magnet incorporated, whereas the hybrid type will be bracketed by conventional chicane magnets.

- The original plan to allow soft switching between normal (i.e. chicane switched off, straight path) and FEMTO mode turned out to be incompatible with the choice of a hybrid type wiggler:
  1. The construction of a vacuum chamber accomodating beams for both geometries, either as a crotched chamber or as a wide open chamber, imposed serious technological problems due to the narrow gap available [7].
  2. Due to the large period length, the residual field of the fully opened wiggler seen by the beam in normal mode is still considerable, i.e. it is not possible to open the wiggler wide enough [5]. Furthermore, since the beam would pass the horizontal field roll-off on a slanting path, it will be affected in a hardly predictable way.

- A horizontal, pure spatial separation was searched in hope that it would allow to reduce the chicane size and with it the emittance increase. However no solution was found. Furthermore, possible problems with the X-ray imaging optics could still not be ruled out even at larger scales than for vertical spatial separation [3].

- The halo problem was investigated [10]. The results do not affect the layout of the insertion but the maximum laser repetition rate and with it the integrated brightness of the FEMTO beamline.

As a consequence of these considerations, a decision was made for the horizontal angular separation scenario and for a non-switchable, but manually unmountable modification of the storage ring.

This paper describes the final design and tries to give a proof, that probably nothing better can be realized given the constraints we have at SLS.

2 Description of layout

As previously documented [9], the FEMTO insertion will be installed in straight 5L of the SLS storage ring. It consists of a modulator wiggler resonant to the short pulse laser beam in order to achieve energy modulation of the electrons in a thin slice of the bunch. The modulator is bracketed by a magnetic chicane to translate the energy modulation of the beam slices into a transverse separation through dispersion. In a radiator undulator, the core beam and the satellites radiate in the X-ray regime. The satellites' radiation leaves the undulator with an inclination angle relative to the beam axis, which is sufficient to allow blocking of the core beam radiation downstream in the beamline and with it clean extraction of the short pulse

X-ray signal. An additional quadrupole triplet located between modulator and radiator creates a sharp focus in the radiator and further provides the necessary degrees of freedom to maintain constraints on betatron phase for preservation of dynamic aperture. Two existing doubletts at the ends of the straights are partially modified to meet the increased requirements on focussing strength.

The chicane/modulator section will be made exchangable for a straight, empty section within a few days, allowing changing between normal and FEMTO geometry during a shutdown week. If it turns out, that the machine can be handled reasonably well in FEMTO mode, and if the unavoidable side-affects are accepted by the non-FEMTO users, the modification may become permanent.

Figure 1 shows the optics of the FEMTO insertion in the SLS storage ring and the figure above table 1 shows the layout.

2.1 Magnets

2.1.1 Changes of ring quadrupoles

The storage ring quadrupole at the radiator side, `QLH-05`, which is of type `QA` with 20 cm length is replaced by a `QB` type with 32 cm length to provide the required focusing strength.

2.1.2 The triplet

The triplet quadrupoles are of same type than the other ring quadrupoles. Basically they could have smaller apertures, but it will be the safer, cheaper and faster solution to use the already well-proven design of the ring quadrupoles instead of developing something new. The triplet quads `QFT1/2/3` will be of type `QBW/QCW/QAW` with 44/32/20 cm length and wide yokes for guiding out the modulator beam. `QAW` however requires a modification since the width of its yoke is insufficient. Probably a new magnet has to be built using the wider iron sheets of `QCW` type for the yoke and installing the `QAW` coils.

2.1.3 Insertion devices

The radiator undulator `U19` is an in-vacuum device similar to the operating `U24` in straight `6S`. It has 95 periods of 19 mm length, an effective field of about 0.94 Tesla and a minimum full gap of 5 mm[6].

The modulator wiggler `W135` probably will be a hybrid device with 17 periods of 135 mm, a peak [effective] field of 1.90 [1.82] Tesla and a full magnet gap of 11 mm, allowing for a vacuum chamber gap of 8 mm (see sect. 3.3 for the constraints on wiggler parameters).

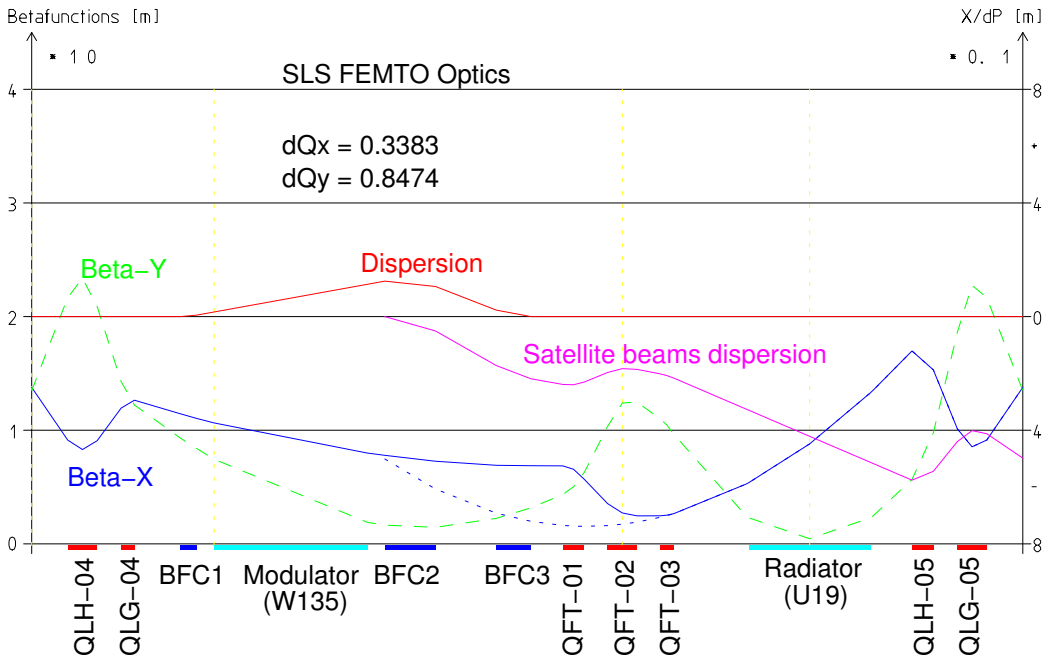

Figure 1: Beam optics of the SLS FEMTO insertion in straight 5L of the SLS storage ring.

2.1.4 Chicane dipoles

The three chicane bending magnets are of conventional type with a moderate field strength. The second chicane magnet BFC2 is comparable to the ring bending magnet type BE. All the three magnets are assumed to be rectangular and aligned parallel to the 5L-axis.

Here are the data of the chicane magnets and a ring TBA end dipole for comparison (a positive angle deflects the beam to the ring outside, i.e. the ring arc dipoles are negative by definition!):

Name	field [T]	arc length [mm]	angle[°]	edge in[°]	edge out [°]
BFC1	1.374	240	2.3620	0.0000	2.3620
BFC2	1.364	760	-7.425	-2.362	-5.063
BFC3	1.359	520	5.063	5.063	0.0000
BE	1.400	800	-8.000	-4.000	-4.000

2.1.5 Distances

The distance between triplet and radiator was maximized for accomodation of the rather bulky modulator absorber. Maximum length was allocated for the modulator in order to increase its length to allow longer periods, and thus decrease its field strength (→ sec.3.3, eq.10). The distances achieved are listed in table 1.

2.2 Matching conditions

Preservation of dynamic aperture requires, that all changes to the lattice are enclosed between the sextupoles `ARIMA-SLB-04/05`, and that the additional betatron phase advances introduced by the FEMTO optics amount to exactly $\Delta\mu_x = 0$, $\Delta\mu_x = \pi$ ("π-trick"). Thus no sextupole "sees" anything from the insertion and dynamic aperture is not affected.

Six of seven degrees of freedom (d.o.f.) provided by the ring quadrupoles `QLG-04/05, QLH-04/05` and the new triplet `QFC1/2/3` are consumed to control the quantities $\beta_x, \alpha_x, \beta_y, \alpha_y$ at the end of the line for maintaining the ring periodicity and for shifting the tune advances, which are $\Delta Q_x = 0.3383, \Delta Q_x = 0.3474$ for the empty straight, to $\Delta Q_x = 0.3383, \Delta Q_y = 0.8474$ in order to acquire exactly the π-shift in vertical betatron phase and nothing horizontally.

The seventh d.o.f. is free and preliminarily used for adjusting $\alpha_y = 0$ in the center of the radiator to obtain the lowest β_y at its edges.

2.3 Restriction of transverse Acceptances

2.3.1 Physical acceptance

The vertical beta at the in-vacuum undulator edges was minimized to $\beta_y = 2.3$ m by adjusting $\alpha_y = 0$ in the undulator centre, reasonably close to the optimum value of $\beta_y = 1.805$ m (= undulator length), which was out of reach. A minimum full gap of 5 mm in `U19` thus restricts the vertical acceptance to 2.7 mm·rad, which is not much less than the present (April 2003) value of 3.1 mm·rad (theoretical value, not yet confirmed by measurements), determined by the wiggler `W61` vacuum chamber (5 mm inner height, 2 m length, $\beta_y = 0.9$ m in the center).

However, the limiting aperture is given by the modulator gap, since the vertical beta function is larger there. The narrow gap of the modulator vacuum chamber has to extend beyond the edges of the magnet array. Assuming a vacuum gap length of 2.5 m (i.e. extending ± 102.5 mm beyond the wiggler edges) and a full vacuum gap height of 8 mm (magnetic gap 11 mm), the vertical acceptance is restricted to 2.05 mm·rad ($\beta_y = 7.82$ m at entrance edge, see fig. 1) in FEMTO mode, resp. to 1.59 mm·rad ($\beta_y = 10.06$ m at entrance edge, see fig. 2) in normal operation, i.e. FEMTO optics switched off but not unmounted.

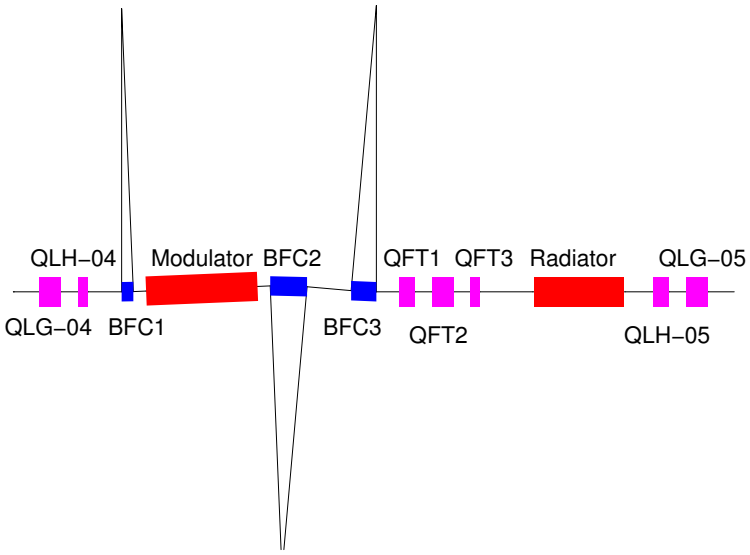

Table 1: Geometry data of FEMTO insertion elements

Location		Path [mm]	X [mm]	Y [mm]	Angle [^{o}]
mid	SLB-04	0.0	0.0	0.0	0.0000
in	QLG-04	540.0	540.0	0.0	0.0000
out	QLG-04	980.0	980.0	0.0	0.0000
in	QLH-04	1340.0	1340.0	0.0	0.0000
out	QLH-04	1540.0	1540.0	0.0	0.0000
in	BFC1	2230.0	2230.0	0.0	0.0000
out	BFC1	2470.0	2469.9	4.9	2.3620
in	W135	2630.0	2629.8	11.5	2.3620
out	W135	5130.0	5127.7	114.6	2.3620
in	BFC2	5290.0	5287.5	121.2	2.3620
out	BFC2	6050.0	6046.8	103.3	-5.0630
in	BFC3	6960.0	6953.2	23.0	-5.0630
out	BFC3	7480.0	7472.6	0.0	0.0000
in	QFT1	7957.4	7950.0	0.0	0.0000
out	QFT1	8277.4	8270.0	0.0	0.0000
in	QFT2	8627.4	8620.0	0.0	0.0000
out	QFT2	9067.4	9060.0	0.0	0.0000
in	QFT3	9417.4	9410.0	0.0	0.0000
out	QFT3	9617.4	9610.0	0.0	0.0000
in	U19	10741.9	10734.5	0.0	0.0000
mid	U19	11653.9	11646.5	0.0	0.0000
out	U19	12565.9	12558.5	0.0	0.0000
in	QLH-05*	13187.4	13180.0	0.0	0.0000
out	QLH-05*	13507.4	13500.0	0.0	0.0000
in	QLG-05	13867.4	13860.0	0.0	0.0000
out	QLG-05	14307.4	14300.0	0.0	0.0000
mid	SLB-05	14847.4	14840.0	0.0	0.0000

2.3.2 Impact on beam lifetime

Elastic scattering lifetime scales with the vertical acceptance. Presently (April 2003) the beam lifetime at 300 mA (in 390 buckets) amounts to approx. 11 h. Presumably, this is composed from 30 h elastic scattering, 48 h bremsstrahlung and 27 h Touschek (third harmonic cavity in operation).

In normal optics mode the modulator gap would halve the elastic scattering lifetime and thus reduce the total lifetime to 9 h. Of course, unmounting the insertion and opening the radiator would avoid lifetime reduction.

In FEMTO mode bunch lengthening is not desired at all and the third harmonic cavity would be switched off or even operated in anti-phase. Without bunch lengthening, Touschek lifetime becomes a third of its value, while the modulator chamber reduces elastic scattering lifetime to 19 h, giving a total lifetime of 4 h. This value would reduce further, if the bunches are compressed. This estimates do not include increase of Touschek lifetime due to emittance blowup from chicane and modulator.

Narrow gaps may potentially reduce Touschek lifetime due to losses from a [coupled] halo, however simulations done for the present lattice configuration did not show any reductions for acceptance restrictions down to 1.1 mm·rad (i.e. 3 mm full gap of 2 m length in a short straight) [11].

After all, the lifetime reduction seems to be acceptable. Anyway, top-up injection makes operation largely independant of lifetime. However increased particle losses still enhance the background radiation.

2.3.3 Rejected alternatives providing larger acceptance

Alternative layouts providing larger vertical acceptance have been considered but did not succeed:

- The modulator could be an electromagnetic superconducting device, which, at this low field, could have a wide gap of approx 20 mm, allowing a warm bore, a massive, simple and robust vacuum chamber. This chamber would allow a sufficient vertical aperture to avoid any lifetime deterioration, and a wide horizontal aperture to accomodate the beam orbits for both normal and FEMTO modes, thus allowing soft switching between the modes by simply pressing a button. However experience with such devices in other places were not generally positive, further the device is expensive and would require a detailed design study which is not compatible with the desired time schedule [5].

- The chicane as shown in fig.1 and in table 1 could be inverted, i.e. `BFT3` and `BFT2` bends would be upstream, `BFT1` downstream the modulator. This required increase of dipole fields by 12 % to 1.55 T (feasible) to obtain the same satellite beam separation as before. Since this layout moves the modulator closer to the centre of the straight, where the vertical betafunction is lower, the

acceptance restriction would be 5.4 mm·rad in FEMTO, resp. 2.57 mm·rad in normal mode. However this inverted chicane does not provide sufficient horizontal separation of the modulator beam from the stored beam axis and thus does not allow to install an absorber between triplet and radiator [7].

2.3.4 Dynamic acceptance

Previous calculations [8] have proven, that there is only little degradation of the machine's dynamic aperture due to the FEMTO insertion. These calculations were done for the old concept of vertical spatial separation, however the insertion devices to be used are basically the same in all schemes. For the modulator even a much stronger device with correspondingly steeper field roll-off had been assumed. The results of this study probably still apply. However, another calculation should confirm that, once the design of the modulator wiggler including multipole contents and field roll-off is known.

2.4 Impact on stored beam parameters

All storage ring radiation equilibrium beam parameters[1] are affected by the insertion :

Natural emittance	5.03 nm·rad	$\rightarrow$	7.34 nm·rad
Momentum compaction	$6.66{\cdot}10^{-4}$	$\rightarrow$	$6.14{\cdot}10^{-4}$
Working point	20.38 / 8.16	$\rightarrow$	20.38 / 8.66
Chromaticities	-65.9 / -20.8	$\rightarrow$	-66.2 / -22.2
Energy loss/turn	512 keV	$\rightarrow$	570 keV
Damping times $x/y/\delta$	9.05 / 9.01 / 4.49 ms	$\rightarrow$	8.13 / 8.10 / 4.04 ms
Circumference	288'000.0 mm	$\rightarrow$	288'007.4 mm
		$\Longrightarrow$	$\Delta f_{RF} = -13$ kHz

Most prominent side-effect is the increase of emittance, which is mainly due to the strong modulator wiggler located in a dispersive region. If the modulator is fully opened (i.e. switched off), the emittance increases to 5.50 nm·rad only, which is the contribution from the chicane magnets alone. Emittance is virtually not affected by the radiator (see sect.3.2 for a detailed analysis and the reason, why this side-effect is unavoidable).

The small increase of chromaticities is easily compensated by the ring sextupole families SF, SD without affecting the dynamic aperture. The required increase in integrated sextupole strength for moving the chromaticities to $(+1/+1)$ is
$(b_3 \cdot L)_{\mathrm{SF}} = 4.248 \rightarrow 4.306\ \mathrm{m}^{-2}$, $\quad (b_3 \cdot L)_{\mathrm{SD}} = -3.950 \rightarrow -4.162\ \mathrm{m}^{-2}$.

[1] The values quoted here are based on an idealized storage ring model with hard edge magnets and ideal magnet lengthes, and agree only on a 5 % level with values obtained from measurements or more detailed models.

The energy loss per turn is higher due to radiation from chicane dipoles and modulator (the modulator wiggler emits a 12 kW X-ray beam [at 400 mA beam current]!). This leads to shorter damping times, which is a pleasant side-effect.

Longer path length due to the excursion in the chicane (see table 1) decreases the radio-frequency significantly and requires retuning of the 2 kHz bandwidth limited BPM electronics.

2.5 Flexibility

2.5.1 Tuning range

The FEMTO optics is taylored to the D2R-optics mode which SLS routinely runs since commissioning. The design working point of $20.38/8.16$ is moved to $20.38/8.66$. The operational range of tune variation of $\approx \pm 0.1/\pm 0.1$ is still available: Tune variation to empirically find the best conditions concerning injection efficiency and lifetime is done by grouping all horizontally and all vertical focussing quadrupoles into two sets and scaling them by a sensitivity matrix obtained from simulations. This procedure of course affects previously defined phase advances, but only to small amounts and in a smooth way and thus does not affect dynamic apertures. In simulation, the same method was proven to work well with the FEMTO insertion too. The tune changes in the FEMTO line are approximately proportional to the total tune change requested. Thus operational flexibility is provided.

2.5.2 Intermediate operation modes

Flexibility to work with incomplete FEMTO operation is shown in figure 2: It is possible to set the lattice to the original tunes, introducing a very small asymmetry in the betafunctions caused by a shift of focal plane in `QLH-05` corresponding to increase of its length to one side by exchanging it for a larger type. In an intermediate mode (year 2004), straight `5L` will run for μXAS experiments using core beam radiation from `U19` while modulator and chicane are not yet installed. For acceptance requirements it will be necessary already then, to shift up the working point in order to obtain a vertical focus in the undulator and with it lowest betafunctions at the edges.

2.5.3 Restriction on optics modes

The FEMTO insertion however does *not* work for the `D1` optics with dispersive straight sections for minimum emittance, since the additional constraints for dispersion matching (η, η') are not covered by the available d.o.f.s.

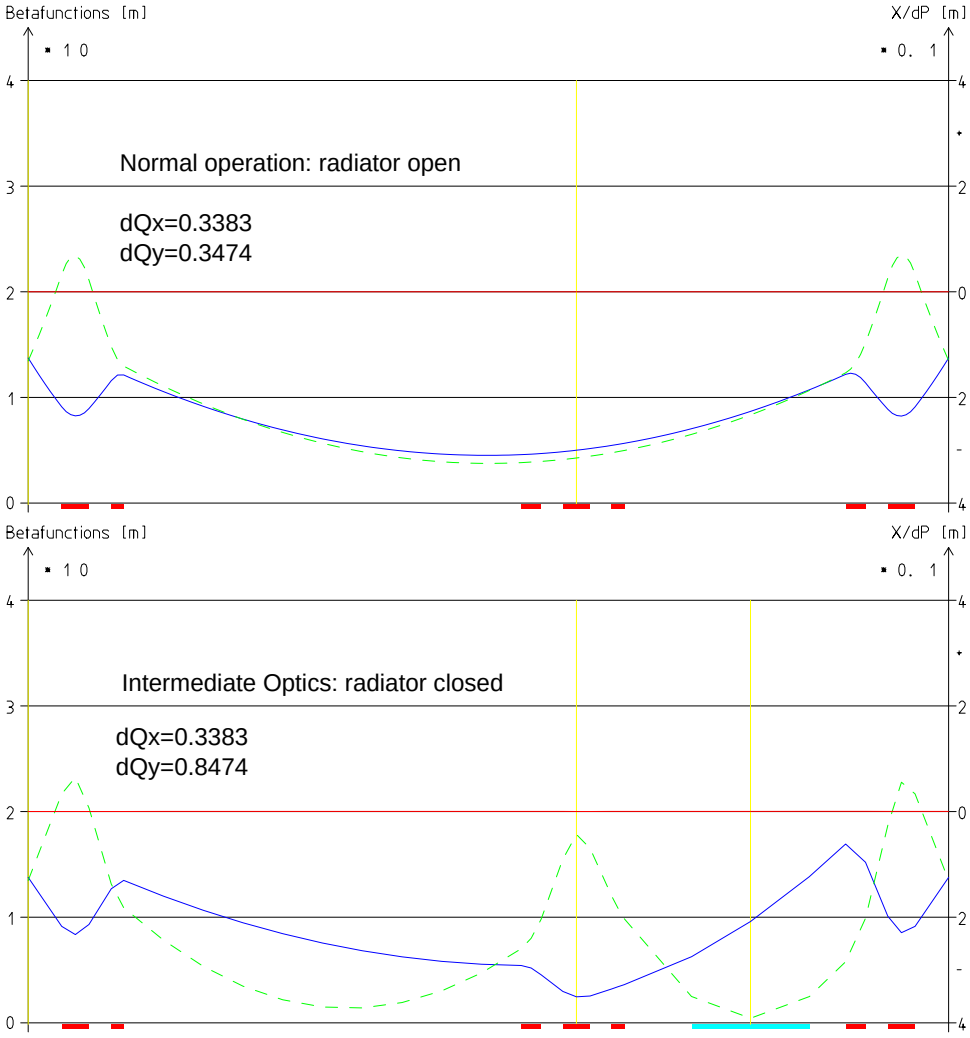

Figure 2: Normal operation with radiator opened (top) and intermediate operation with radiator closed but modulator and chicane not yet installed or temporarily removed (bottom). (β_x solid, β_y dashed).

2.6 Performance

Assuming a laser providing an energy modulation of 13 Mev absolute or $5.4{\cdot}10^{-3}$ relative, the satellite beams at the radiator center will be separated in position and angle by

$$\boxed{\pm x_1 = -2.22 \text{ mm} \qquad \pm x_1' = -0.53 \text{ mrad}}$$

At a location 15 m downstream the corresponding photon beams arrives at ∓ 10 mm displacement. Thus a blade 7 mm off-axis blocks the core beam, the positive satellite beam, the radiation from ring dipoles, modulator and chicane and extracts almost all the radiation from the negative satellite beam.

The integrated brightness of the system depends on the slicing efficiency, which amounts to $4.3{\cdot}10^{-4}$ (see [9], sec.2.2.3) and on the laser repetition rate which, in order to avoid any halo background, is restricted to $M{\cdot}200$ Hz when working with M bunches and $480/M$ ns shutters or gates [10], where $M \approx 8$ seems feasible[2]. Thus the brightness in FEMTO-mode is smaller compared to the normal mode by a factor composed from slicing efficiency and the ratio of laser repetition rate to revolution frequency, its value given by $8{\cdot}M \cdot 10^{-8}$.

3 How beam separation is connected with emittance increase

3.1 Beam separation

The dispersion at the modulator center considered as location of laser interaction (actually the interaction extends over all the modulator) is given by

$$\eta_o = \rho_1 \cdot (1 - \cos\phi_1) + L_{1m}\eta_o' \qquad \eta_o' = \sin\phi_1 \tag{1}$$

with ϕ_1, ρ_1 deflection angle and radius of the first chicane bending magnet and L_{1m} the distance between its exit edge and the modulator center. The betatron amplitude of the satellite beams generated by laser induced energy change $\pm\hat{\delta}$ at the modulator center is invariant between bends (neglecting small dispersion variations due to the wiggler poles) and thus at any location inside the modulator given by

$$H_w \cdot \hat{\delta}^2 \quad \text{with} \quad H = \gamma\eta^2 + 2\alpha\eta\eta' + \beta\eta'^2. \tag{2}$$

The transformation from modulator center ("0") to radiator center ("1") is given by a 3×3 matrix M, which has the property to close the dispersion bump by means of the second and third chicane magnets:

$$M = \begin{pmatrix} C & S & D \\ C' & S' & D' \\ 0 & 0 & 1 \end{pmatrix} \qquad M \cdot \begin{pmatrix} \eta_o \\ \eta_o' \\ 1 \end{pmatrix} = \begin{pmatrix} 0 \\ 0 \\ 1 \end{pmatrix} \quad \Longrightarrow \quad \begin{array}{c} D = -\eta_o C - \eta_o' S \\ D' = -\eta_o C' - \eta_o' S' \end{array}$$

[2]These calculations however were rather pessimistic since they did not include the acceptance limitations of the beamline which may help to suppress the background significantly.

Considering particles of some energy deviation δ' and negligible transverse coordinates, we can show, that the satellite beams are *not* blown up due to dispersion, they just receive an offset[3]:

$$\begin{pmatrix} x \\ x' \\ \delta \end{pmatrix}_1 = M \begin{pmatrix} \eta_o\delta' \\ \eta_o'\delta' \\ \delta' \pm \hat{\delta} \end{pmatrix} = \begin{pmatrix} D\hat{\delta} \\ D'\hat{\delta} \\ \delta' \pm \hat{\delta} \end{pmatrix} = \pm \begin{pmatrix} \begin{pmatrix} C & S \\ C' & S' \end{pmatrix} \begin{pmatrix} \eta_o \\ \eta_o' \end{pmatrix} \\ 1 \end{pmatrix} \hat{\delta} + \begin{pmatrix} 0 \\ 0 \\ \delta' \end{pmatrix}$$

The submatrix for betatron motion is expressed conveniently by local normalizations and a rotation about the betatron phase advance Φ:

$$\begin{pmatrix} C & S \\ C' & S' \end{pmatrix} = T_1^{-1} \cdot \begin{pmatrix} \cos\Phi & \sin\Phi \\ -\sin\Phi & \cos\Phi \end{pmatrix} \cdot T_o \quad \text{with} \quad T = \begin{pmatrix} 1/\sqrt{\beta} & 0 \\ \alpha/\sqrt{\beta} & \sqrt{\beta} \end{pmatrix}$$

Using T_o the dispersion of the sliced beams can be normalized to assign an initial betatron phase Ψ to the satellite beams:

$$T_o \begin{pmatrix} \eta \\ \eta' \end{pmatrix}_o = \sqrt{H_w} \cdot \begin{pmatrix} \cos\Psi \\ \sin\Psi \end{pmatrix} \quad \text{with} \quad \Psi = \pi + \arctan\left(\alpha_o + \beta_o \frac{\eta_o'}{\eta_o}\right)$$

The offset of π in Ψ is due to the fact, that the laser interaction changes the *energy* of the particles and with it the center of further betatron motion, whereas the transverse position itself is *not* changed.

Propagating further to the radiator center requires rotation by Φ and backtransformation T_1^{-1} and finally gives for the separation of the satellites

$$\pm \begin{pmatrix} x \\ x' \end{pmatrix}_1 = \begin{pmatrix} \eta \\ \eta' \end{pmatrix}_1 \hat{\delta} = \sqrt{H_w} \cdot \hat{\delta} \cdot \begin{pmatrix} \sqrt{\beta} & 0 \\ -\alpha/\sqrt{\beta} & 1/\sqrt{\beta} \end{pmatrix}_1 \cdot \begin{pmatrix} \cos(\Psi - \Phi) \\ \sin(\Psi - \Phi) \end{pmatrix} \quad (3)$$

3.1.1 Approximations

Considering the particular situation for SLS-FEMTO which is rather constrained, we may introduce several approximations to better understand how the separation of the beams is optimized.

For the kind of optics we consider, it turns out, that $(\Psi - \Phi) \approx \pi$. Thus eq.3 simplifies to

$$x_1 \approx 0 \qquad \pm x_1' \approx -\sqrt{H_w}\,\hat{\delta}\,\frac{\alpha_1}{\sqrt{\beta_1}}$$

This explains why attempts to design a pure spatial separation scheme with large $\pm x_1$ and $x_1' \approx 0$ did not succeed. We may simplify further assuming a kind of virtual focus in distance L^* upstream the radiator centre (shown by the dotted line in fig.1):

$$\alpha^* = 0 \qquad \beta^* = \frac{\beta_1}{1+\alpha_1^2} \qquad L^* = -\alpha_1\beta^*,$$

[3]This was wrong in [9], sections 2.2.4 and 4.1.3

for $\beta^* \ll L^*$ eventually arriving at the approximate expression

$$\pm x_1' \approx \sqrt{\frac{H_w}{\beta^*}}\,\hat{\delta} \tag{4}$$

This is still not the end, since a large beta-function in the modulator made the third term in eq.2 dominate (contributes ≈ 80 %), thus using eq.1 and $\phi_1 \ll 1$ we further simplify to

$$\pm x_1' \approx \phi_1 \hat{\delta} \sqrt{\frac{\beta_o}{\beta^*}}.$$

This result still agrees on a 20 % level with the exact calculation of eq.3 and reveals the means how to optimize the angle of separation:

- large angle of the first chicane magnet,
- obviously a strong laser ,
- large horizontal beam size in the modulator,
- sharp virtual focus inside the triplet.

3.2 Wiggler emittance contributions

A wiggler in a dispersive section changes (increases or decreases) the total emittance by a factor [1]

$$\frac{\varepsilon_w}{\varepsilon_o} = \frac{1 + \frac{I_5^w}{I_5^o}}{1 + \frac{I_2^w}{I_2^o}} \tag{5}$$

with ε_w, ε_o the emittance with and without wiggler, where ε_o is given by

$$\varepsilon_o = 3.84 \cdot 10^{-4}\,[\text{nm·rad}]\,\frac{\gamma^2 I_5^o}{J_x I_2^o} \tag{6}$$

and the synchrotron integrals given by

$$I_2 = \oint \frac{1}{\rho^2}\,ds \qquad I_5 = \oint \frac{H}{|\rho^3|}\,ds, \tag{7}$$

where superscripts o and w in eq.5 indicate that the integrals are to be taken over only the bending magnets, resp. over only the wiggler.

For SLS at 2.4 GeV with 1.4 T bending field tuned to the standard "D2R" optics providing $\varepsilon_o = 5.03$ nm·rad, the ring integrals are given by ($J_x \approx 1$ since the bends have no gradients)

$$I_2^o = 1.0965\,\text{m}^{-1} \qquad I_5^o = 6.5106 \cdot 10^{-4}\,\text{m}^{-1}$$

The variation of the H-function inside the wiggler is negligible compared to its

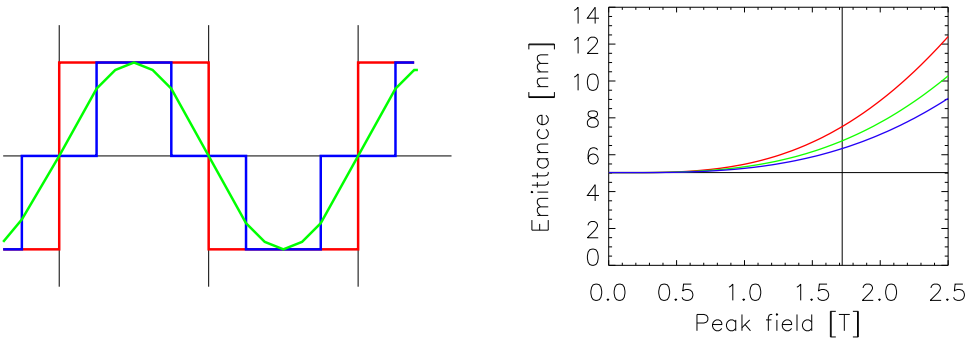

Figure 3: Emittance increase in SLS due to modulator wiggler as a function of wiggler peak field for different forms of field variation, chicane magnets' contribution not included.

value created by the first chicane magnet, thus it is treated as a constant H_w and the wiggler integrals give

$$I_2^w = \begin{bmatrix} 1 \\ 1/2 \\ 1/2 \end{bmatrix} \cdot L_w \left(\frac{\hat{B}}{B\rho}\right)^2, \quad I_5^w = \begin{bmatrix} 1 \\ 2/\pi \\ 1/2 \end{bmatrix} \cdot L_w H_w \left(\frac{\hat{B}}{B\rho}\right)^3 \quad \text{for} \begin{bmatrix} \text{full} \\ \text{sine} \\ \text{half} \end{bmatrix} \text{poles} \tag{8}$$

as sketched in fig.3 (left). With the chicane as described above providing $H_w = 0.0186$ m·rad and assuming a wiggler of length 2.3 m (17×0.135 m), the resulting emittance increase as a function of wiggler peak field $\hat{B}$ is plotted in fig.3 (right). This does not include contributions from the chicane magnets which amount to $\Delta\varepsilon_{\text{chicane}} \approx 0.5$ nm·rad. The final wiggler design has not yet been chosen. With a peak field of about 1.9 Tesla and a most likely tapezoidal field variation which would give slightly larger integrals than the sinusoidal field, we thus have to expect an emittance ε_w of $7 \ldots 8$ nm·rad.

Examining the range of numbers for SLS-FEMTO, it turns out that I_2^w is less than 10 % of I_2^o, and eq.5 can be simplified to estimate the relative increase of emittance:

$$\frac{\Delta\varepsilon_w}{\varepsilon_o} \approx \frac{I_5^w}{I_5^o} = k f L_w H_w \hat{B}^3 \quad \text{with} \quad k := (B\rho)^3 I_5^o \approx 3\,\text{T}^3\text{m}^2 \quad \text{forSLS} \tag{9}$$

and f the formfactor for I_5^w depending on the field shape as given in eq.8.

3.3 Constraints on the wiggler[5]

The laser for slicing will operate at 800 nm wavelength and at a pulse duration (FWHM) of 50 fs which corresponds to 18 optical cycles. The pulse energy re-

quirement of about 5 mJ is the most challenging constraint and prohibits to go to lower wavelength. This defines the wiggler parameters:

First, the laser has to be resonant with the wiggler:

$$\lambda_L = \frac{\lambda_w}{2\gamma^2}\left(1+\frac{K_w^2}{2}\right), \quad \text{with} \quad K_w = \frac{e}{2\pi m_o c}\lambda_w \hat{B}$$

for a sinuisodal field shape. Since $K_w \gg 1$ in case of a wiggler, we may write

$$\lambda_w^3 \hat{B}^2 \approx \lambda_L \left(\frac{4\pi m_o c\gamma}{e}\right)^2 \approx 0.008\,\mathrm{m^3T^2} \quad \text{for SLS-FEMTO} \tag{10}$$

Second, the number of wiggler periods N_w should equal the number of optical cycles to obtain full modulation of the electron beam.

$$N_w = L_w/\lambda_w \approx 18 \quad \text{for SLS-FEMTO}$$

In order to keep the peak field as low as possible to limit emittance increase according to eq.9, the period should be as long as possible, however is limited by the available length for the modulator, since the number of periods is given. Thus the wiggler dimensioning will rather proceed the other way round: Take all available space, divide it by ≈ 18 to get the period and set the peak field according to eq.10. In this way, the initial design of a 2.5 T wiggler with 110 mm periods was changed to a 1.9 T wiggler with 135 mm periods.

Coming back to eq.9 we insert eq.4 to eliminate H_w and get, assuming a sinusoidal field shape,

$$\frac{\Delta\varepsilon_w}{\varepsilon_o} \approx \frac{2\,k}{\pi\hat{\delta}^2} \cdot L_w \hat{B}^3 \cdot \beta^* x_1'^2$$

The wiggler was already optimized for lowest peak field, as mentioned above. A certain value of angular separation is required to extract the satellite radiation. The triplet focusing to provide low β^* reaches limits due to the requirement to keep the horizontal phase advance constant over the insertion. The pulse energy of the slice laser would be the most efficient parameter to lower the emittance increase (providing a higher value of $\hat{\delta}$ allowing to scale down the chicane), however the proposed values are already at the edge of technology.

Thus, **the increase of emittance can not be avoided**.

Inserting some reasonable numbers as
$\hat{\delta} = 0.54\,\%$ $L_w = 2.3$ m $\hat{B} = 1.9$ T $\beta^* = 1.5$ m $x_1' = 0.5$ mrad
a 30…40 % emittance increase from the wiggler has to be accepted. Another ≈10 % come from the chicane magnets.

References

[1] A.W.Chao, M.Tigner, Handbook of accelerator physics and engineering, Singapore 1998

[2] Calculation results from O.Chubar, G.Ingold, priv.comm.

[3] D.Grolimund, priv. comm.

[4] G.Ingold et al, Sub-picosecond optical pulses at the SLS storage ring, PAC-01, Chciago, June 2001.

[5] G.Ingold, priv.comm.

[6] G.Ingold, Status: Undulator X-ray source for time resolved ps- and sub-ps pump-probe experiments in the range 5-18 keV, PSI Annual report 2003

[7] L.Schulz, priv.comm.

[8] B.Singh, SLS storage ring non-linear dynamics with FEMTO insertion in one straight section,SLS-TME-TA-2001-0181

[9] A.Streun, Some considerations on the SLS FEMTO insertion, SLS-TME-TA-2002-0199

[10] A.Streun, SLS-FEMTO: Beam halo formation and maximum repetition rate for laser slicing, SLS-TME-TA-2003-0222

[11] A.Streun, Beam lifetime in the SLS storage ring, SLS-TME-TA-2001-0191

A Final Geometry and Optics of the SLS FEMTO Insertion

Addendum to SLS-TME-TA-2003-0223 from May 1st, 2003
Andreas Streun, June 17th, 2004

A.1 Erratum

In SLS-TME-TA-2003-0222/0223 the sign of dispersion was wrong *everywhere*. Dispersion defined as $x/(\Delta E/E)$ is *negative*, if the particles with *lower* energy are travelling at the ring *outside*, as it is the case in the FEMTO chicane, whereas it is positive in the arcs. As a consequence, the FEMTO satellite with *positive* energy modulation is the one, which emits its light to the ring outside and along the FEMTO beamline. All numbers are still correct in absolute value, but all signs have to be changed.

A.2 Changes of layout

During the engineering process of the FEMTO insertion [L.Schulz, A.Keller], some technical limitations led to modifications of the final design:

The quadrupole QLH-05 was shifted downstream by 100 mm, thus reducing the distance to QLG-05 from 360 mm to only 260 mm. This restricts the margin for matching the optics and increases the current of the quadrupoles.

The first chicane magnet BFC1 was increased in length from 240 mm to 320 mm for reasons of field homogeneity. Subsequently, the chicane geometry was slightly changed and the angles of BFC2 and BFC 3 had to be adjusted:

Name	field [T]	arc length [mm]	angle[°]	edge in[°]	edge out [°]
BFC1	1.031	320.0	2.3620	0.0000	2.3620
BFC2	1.359	753.7	-7.3462	-2.362	-4.9842
BFC3	1.359	512.1	4.9842	4.9842	0.0000

Table 2 gives the final geometry (compare with table 1).

A.3 FEMTO optics modes

For the optics, two modes with different advantages were found and named F6C1 and F6C2. The optical functions are shown in figure 4 (top) – compare to figure 1.

The most important parameters of the two modes and of the previous F4C mode are compared in the following table:

	Optics mode	F4C	F6C1	F6C2
Spatial beam separation	Δx [mm]	2.20	2.19	2.13
Angular beam separation	$\Delta x'$ [mrad]	0.53	0.46	0.51
Vert. acc. restriction from Mod.	A_y^{mod} [mm mrad]	2.00	2.12	1.98
Vert. acc. restriction from Rad.	A_y^{rad} [mm mrad]	2.51	2.12	2.50
Maximum quadrupole current	$I_{\mathrm{QLG-05}}$ [A]	110.0	114.2	117.0
Ring equilibrium emittance	ϵ_{xo} [nm rad]	7.30	7.20	7.28
RF detuning for increased path	Δf_{rf} [kHz]	-12.9	-12.5	-12.5

All data are for 2.4 GeV beam energy. Beam separation was calculated for $\Delta E/E = 5.4 \cdot 10^{-3}$ energy modulation. Acceptance also includes a pipe/flange in front of the modulator of 100 mm length. Modulator and radiator have full vacuum gaps of 8 mm, resp. 5 mm.

Optics F6C1 is better concerning vertical acceptance, providing same restrictions from the modulator entry edge and the radiator exit edge. $\alpha_y \neq 0$ in the radiator center but small. The third triplet quadrupole QFT3 is switched off. Tunes, alphas and betas were matched using the six remaining quadrupoles. The maximum quadrupole current is lower, but the beam separation is smaller.

Optics F6C2 provides better beam separation, but on expense of a rather high current in QLG-05. Now all seven quads were used with the additional constraint $\alpha_y = 0$ in the radiator centre. β_y at the modulator entrance edge is slightly larger, leading to a reduced vertical acceptance.

The QLG-05 current close to the present 120 A highest operating value of the power supply calls for an upgrade of QLG-04/-05 to 140 A (as already done for all QSF, QMF and QLH supplies in view of future 2.7 GeV operation [M.Horvat]). This also would allow FEMTO operation at 2.7 GeV with currents of 133.3 A (QLG-05), resp. 129.8 A (QLG-04).

As an intermediate setting before modulator installation, the optics F6T was calculated, similar to the presently operating F4T optics.

An optics without radiator and modulator taking back the $\Delta Q_y = 0.5$ tune shift, was also established and named F60, although it probably will never be used. In contrary to the corresponding F40 optics, it was necessary to power slighly the triplet quadrupoles for proper tune matching. Both optics are shown in figure 4 (bottom).

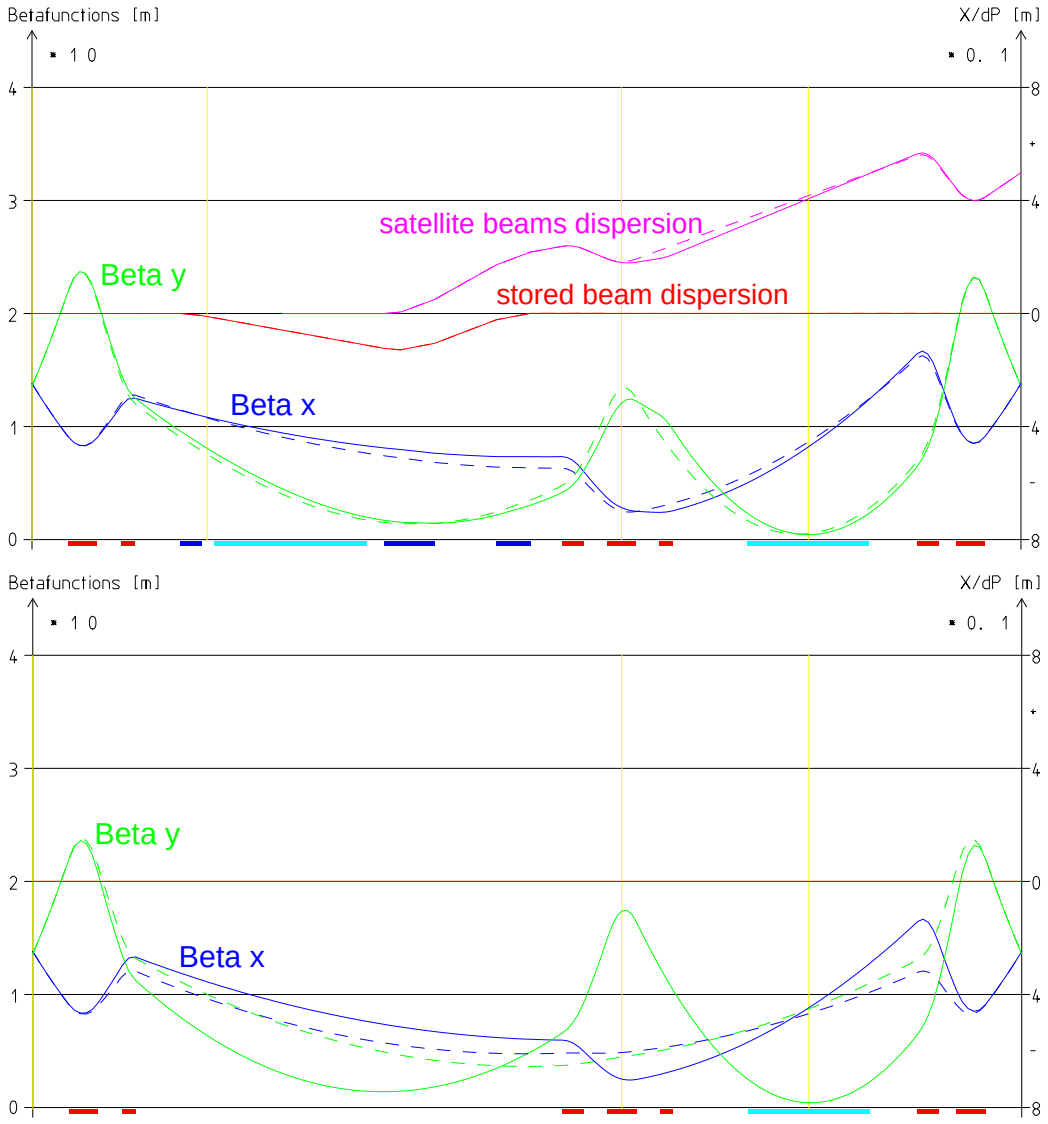

Figure 4: FEMTO optics

Top: Solutions F6C1 (dashed) and F6C2 (solid) for the beam optics of the SLS FEMTO insertion in straight 5L of the SLS storage ring.
Bottom: Solutions F6T (solid) and F60 (dashed) for the beam optics of the 5L straight before chicane installation, resp. for the empty straight. For magnet names see fig.1.

Table 2: Geometry data of FEMTO insertion elements

Location		Path [mm]	X [mm]	Y [mm]	Angle [^{o}]
mid	SLB-04	0.0	0.0	0.0	0.0000
in	QLG-04	540.0	540.0	0.0	0.0000
out	QLG-04	980.0	980.0	0.0	0.0000
in	QLH-04	1340.0	1340.0	0.0	0.0000
out	QLH-04	1540.0	1540.0	0.0	0.0000
in	BFC1	2220.0	2220.0	0.0	0.0000
out	BFC1	2540.0	2539.9	6.6	2.3620
in	W135	2630.0	2629.8	10.3	2.3620
out	W135	5130.0	5127.7	113.3	2.3620
in	BFC2	5290.0	5287.6	119.9	2.3620
out	BFC2	6044.7	6041.6	102.7	-4.9842
in	BFC3	6970.3	6963.6	22.3	-4.9842
out	BFC3	7482.4	7475.1	0.0	0.0000
in	QFT1	7957.4	7950.0	0.0	0.0000
out	QFT1	8277.4	8270.0	0.0	0.0000
in	QFT2	8627.4	8620.0	0.0	0.0000
out	QFT2	9067.4	9060.0	0.0	0.0000
in	QFT3	9417.4	9410.0	0.0	0.0000
out	QFT3	9617.4	9610.0	0.0	0.0000
in	U19	10700.4	10693.0	0.0	0.0000
mid	U19	11653.9	11646.5	0.0	0.0000
out	U19	12607.4	12600.0	0.0	0.0000
in	QLH-05	13287.4	13280.0	0.0	0.0000
out	QLH-05	13607.4	13600.0	0.0	0.0000
in	QLG-05	13867.4	13860.0	0.0	0.0000
out	QLG-05	14307.4	14300.0	0.0	0.0000
mid	SLB-05	14847.4	14840.0	0.0	0.0000